



OPEN

# A novel transgenic mouse strain expressing PKC $\beta$ II demonstrates expansion of B1 and marginal zone B cell populations

Ali A. Azar<sup>1,4</sup>, Alison M. Michie<sup>1b2</sup>, Anuradha Tarafdar<sup>2</sup>, Natasha Malik<sup>1b2</sup>, Geetha K. Menon<sup>3</sup>, Kathleen J. Till<sup>1</sup>, Nikolina Vlatković<sup>1,5✉</sup> & Joseph R. Slupsky<sup>1b,5✉</sup>

Protein kinase C $\beta$  (PKC $\beta$ ) expressed in mammalian cells as two splice variants, PKC $\beta$ I and PKC $\beta$ II, functions in the B cell receptor (BCR) signaling pathway and contributes to B cell development. We investigated the relative role of PKC $\beta$ II in B cells by generating transgenic mice where expression of the transgene is directed to these cells using the E $\mu$  promoter (E $\mu$ -PKC $\beta$ IItg). Our findings demonstrate that homozygous E $\mu$ -PKC $\beta$ IItg mice displayed a shift from IgD<sup>+</sup>IgM<sup>dim</sup> toward IgD<sup>dim</sup>IgM<sup>+</sup> B cell populations in spleen, peritoneum and peripheral blood. Closer examination of these tissues revealed respective expansion of marginal zone (MZ)-like B cells (IgD<sup>+</sup>IgM<sup>+</sup>CD43<sup>neg</sup>CD21<sup>+</sup>CD24<sup>+</sup>), increased populations of B-1 cells (B220<sup>+</sup>IgD<sup>dim</sup>IgM<sup>+</sup>CD43<sup>+</sup>CD24<sup>+</sup>CD5<sup>+</sup>), and higher numbers of immature B cells (IgD<sup>dim</sup>IgM<sup>dim</sup>CD21<sup>neg</sup>) at the expense of mature B cells (IgD<sup>+</sup>IgM<sup>+</sup>CD21<sup>+</sup>). Therefore, the overexpression of PKC $\beta$ II, which is a phenotypic feature of chronic lymphocytic leukaemia cells, can skew B cell development in mice, most likely as a result of a regulatory influence on BCR signaling.

B cell receptor (BCR) signaling plays an essential role at critical stages of B cell development<sup>1,2</sup>. In the bone marrow spontaneous and environmental ligand-induced tonic signals from this receptor aid the transition of developing B cells from one stage of differentiation to the next until they emerge into peripheral circulation. In the periphery, mature B cells move between secondary lymphoid organs where specific antigen recognition by BCR results in their activation and differentiation to ultimately generate cells that yield specific antibody production and immune memory. Key signaling molecules have been found to be intricately linked to the stage specific responses of BCR signaling. While this is particularly true for the early stages of B cell differentiation where this relationship is well defined, the roles of signaling molecules involved in B cell fate decisions in the periphery are less well characterized and understood<sup>2</sup>.

One such signaling molecule is Protein kinase C $\beta$  (PKC $\beta$ ), which plays a central role in the appropriate regulation of B cell development and activation, including BCR signaling<sup>3</sup>. It has been demonstrated that knock-down of the PKC $\beta$  gene, *prkcb*, in mice results in immunodeficiency that is reminiscent of X-linked immunodeficiency, and corresponds to impaired humoral immune responses and B cell function<sup>4</sup>. PKC $\beta$  plays an important role in B cell development and activation, including BCR signaling<sup>3,4</sup>.

A key target of PKC $\beta$  during BCR engagement is Bruton's tyrosine kinase (Btk). PKC $\beta$  phosphorylates Btk to provide feedback inhibition of BCR signaling by blocking its ability to activate phospholipase C $\gamma$ 2 (PLC $\gamma$ 2) and stimulate Ca<sup>2+</sup> release from intracellular stores<sup>5</sup>. Genetic studies have confirmed a functional relationship between PKC $\beta$  and Btk, showing that there is great similarity of B cell-related phenotypes resulting from targeted disruption of the genes coding for these proteins<sup>4,6-8</sup>. The gene coding for PKC $\beta$ , *PRKCB*, when transcribed is alternatively spliced to yield PKC $\beta$ I and PKC $\beta$ II, which differ from each other within their C-terminal 50 amino

<sup>1</sup>Department of Molecular and Clinical Cancer Medicine, University of Liverpool, 1st Floor Sherrington Building, Ashton Street, Liverpool L69 3GE, UK. <sup>2</sup>Molecular Lymphopoiesis Group, Institute of Cancer Sciences, College of Medical, Veterinary and Life Sciences, University of Glasgow, Glasgow, UK. <sup>3</sup>Department of Histopathology, Royal Liverpool University Hospital, Liverpool, UK. <sup>4</sup>Present address: Barts Cancer Institute, Barts and the London School of Medicine and Dentistry, Queen Mary University of London, London, UK. <sup>5</sup>These authors contributed equally: Nikolina Vlatković and Joseph R. Slupsky. ✉email: vlatko@liverpool.ac.uk; jslupsky@liverpool.ac.uk

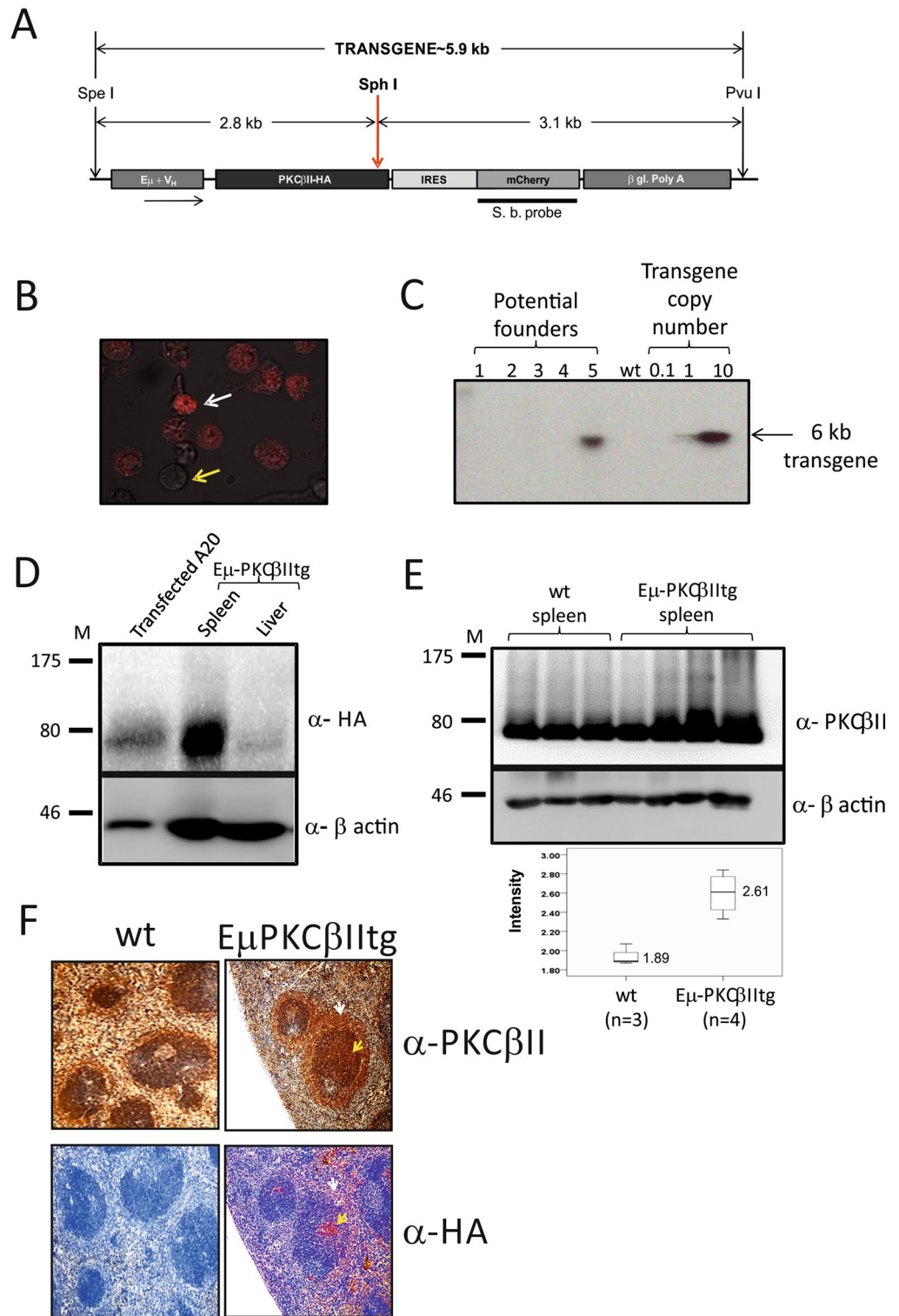
**Figure 1.** Generation of  $\text{E}\mu\text{-PKC}\beta\text{II}$  transgenic mice. **(A)** Schematic representation of the plasmid construct (p $\text{E}\mu\text{-PKC}\beta\text{II-IRES-mCherry}$ ) used to generate transgenic mice. **(B)** A20 cell line transfected with p $\text{E}\mu\text{-PKC}\beta\text{II-IRES-mCherry}$  plasmid using nucleofection. White arrow indicates fluorescent A20 cells that were successfully transfected and express mCherry. Yellow arrow indicates those cells which did not take up the plasmid. **(C)** Southern blot analysis of genomic DNA isolated from tail cuttings of transgenic progeny to identify potential  $\text{E}\mu\text{-PKC}\beta\text{II}$  founder mice. Copy number of the inserted gene was estimated by the accompanying standard curve of plasmid DNA. **(D)** Immunoblot analysis of protein extracted from splenic and liver tissue of homozygous  $\text{E}\mu\text{-PKC}\beta\text{II}$  mice. Western blots were performed using antibodies against HA (*upper panel*) or  $\beta$ -actin (*lower panel*). As positive control, protein lysates prepared from A20 cells that had been transiently transfected with p $\text{E}\mu\text{-PKC}\beta\text{II-IRES-mCherry}$ . **(E)** *Upper and middle panel.* Respective western blot analysis of PKC $\beta\text{II}$  and  $\beta$ -actin expression in splenic tissue of wt ( $n=3$ ) and  $\text{E}\mu\text{-PKC}\beta\text{II}$  ( $n=4$ ) mice. *Lower panel.* Comparison of PKC $\beta\text{II}$  expression in wt and  $\text{E}\mu\text{-PKC}\beta\text{II}$  mice. Expression of PKC $\beta\text{II}$  was quantitated relative to  $\beta$ -actin. **(F)** Immunohistochemical staining of spleen sections from  $\text{E}\mu\text{-PKC}\beta\text{II}$  and wt mice with anti-HA (stained with Fast Red) and anti-PKC $\beta\text{II}$  antibodies (brown with DAB). With respect to  $\text{E}\mu\text{-PKC}\beta\text{II}$  mice, the spleen sections are sequential where upper and lower images can be superimposed using the white arrow which points to the MZ and the yellow arrow which points to the follicle. The images in parts (C–E) have been cropped to efficiently show the relevant details, uncropped images can be viewed in the Supplementary information accompanying this manuscript. All elements of this figure have been published in the PhD thesis of AAA<sup>43</sup>.

acids<sup>9,10</sup>. However, it is not clear whether these isoforms have redundant or specific functions in B cell development and activation.

Our previous studies of PKC $\beta\text{II}$  in the malignant cells of B lymphoproliferative disorders have shown that overexpression of this PKC isoform is a phenotypic feature of chronic lymphocytic leukaemia (CLL) cells<sup>11</sup>. In addition, the Tc11-transgenic mouse model of CLL demonstrates that PKC $\beta$  plays a key role in the pathogenesis of CLL, because PKC $\beta$  deficient mice do not develop CLL-like disease<sup>12</sup>. One possible explanation for this is the severe reduction in numbers of marginal zone B cells (MZ B cells) and B-1 B cells in PKC $\beta$  knock out mice<sup>4</sup>, since these are the cells from which CLL is thought to arise<sup>13,14</sup>. Interestingly, in virtually all mouse models of CLL, malignant cells develop from an expanded B-1 B cell compartment<sup>15–19</sup>, and this is similar to human disease which is preceded by a condition known as monoclonal B lymphocytosis<sup>20</sup>. Based on these combined findings, we wanted to investigate the effect of PKC $\beta\text{II}$  overexpression in the B cell compartment. Considering the role of PKC $\beta$  in modulating BCR signaling and in B cell development, particularly the development of B-1 and MZ B cells, we hypothesized that transgenic expression of PKC $\beta\text{II}$  within B cells of mice might lead to an expansion in populations of these B cell types.

## Materials and methods

**Generation of the  $\text{E}\mu\text{-PKC}\beta\text{II}$  tg mice.** To generate  $\text{E}\mu\text{-PKC}\beta\text{II}$  mice, a pSVE6BK plasmid (kindly provided by Dr. Raif Geha, Harvard Medical School) which exploits the VH promoter and the IgH-enhancer to specifically direct expression of target genes in B cells was used (p $\text{E}\mu$  vector<sup>21</sup>). The full length PKC $\beta\text{II}$  coding sequence (2021-bp) was tagged with human influenza HA at its 3' end by PCR, using the forward 5'-GAGAATCGATCAAGATG-GCTGACCCGGCTGCGGGGCC-3', and the reverse 5'-GAGAGTCGACTCAAAGAGCGT AATCTGGAACATCGTATGGGTAGCTCTTGACTTCGGGTTTTAAA-3' primers (Eurofins MWG Operon, London UK) prior to cloning into the ClaI (all restriction enzymes used in this study are from New England Biolabs, Hitchin UK) and SalI sites of the p $\text{E}\mu$  vector. An intra-ribosomal entry site (IRES) was sub-cloned into the BamHI and SalI sites of the multiple cloning site (MCS) of mCherry, and the IRES-mCherry coding sequence was then sub-cloned into p $\text{E}\mu\text{-PKC}\beta\text{IIHA}$  using Not-I and Apa-I placing it in a 5'→3' unilateral orientation between the PKC $\beta\text{IIHA}$  and  $\beta$ -poly-globin coding sequences in the  $\text{E}\mu$  vector (Fig. 1A). This construct was tested in the mouse B lymphoma cell line A20<sup>22</sup> where  $2 \times 10^6$  cells were nucleofected<sup>™</sup> with 2  $\mu\text{g}$  p $\text{E}\mu\text{-PKC}\beta\text{IIHA-IRES-mCherry}$  using the solution V transfection kit and programme U-013 according to the manufacturer's protocol (Lonza, Tewkesbury, UK) and fluorescence associated with the expression of mCherry observed (Fig. 1B). The construct containing p $\text{E}\mu\text{-PKC}\beta\text{IIHA-IRES-mCherry}$  was then digested with Pvu-I and Spe-I, DNA fragment purified and injected into pronuclei of zygotes isolated from C57Bl/CBA F1 hybrid mice. Mice generated from this procedure were screened for the presence of the transgene by Southern blot analysis on genomic DNA isolated from the tail and digested with SphI. Blots were hybridized with the mCherry specific DNA probe labeled with <sup>32</sup>P-dCTP (Amersham Megaprime DNA Labelling System), essentially as described previously<sup>23</sup>. Founders were identified by higher expression, and/or evidence of a single integration site for the transgene (Fig. 1C), and those showing transgene integration in their genome were chosen for further breeding to generate the heterozygous and ultimately homozygous  $\text{E}\mu\text{-PKC}\beta\text{II}$  transgenic animals that were analysed in this study. To establish the first-generation of  $\text{E}\mu\text{-PKC}\beta\text{II}$  heterozygous mice, the founder mouse was back-crossed with C57Bl/6 wild type mice to generate F1 progeny. The heterozygous mice from this crossing were then selected and inter-crossed to generate F2 progeny. Some of these F2 mice were homozygous, and, at this point, we reconsidered the line established and these mice were used for phenotypical characterization as well as for breeding to expand the line.  $\text{E}\mu\text{-PKC}\beta\text{II}$ , littermate wt and non-littermate control mice were all maintained under identical conditions. Mice were generated and bred in-house within the Biological Services Units at the University of Liverpool and the University of Glasgow. Animal experiments were performed with appropriate approval and licenses from the UK Home Office. All experimental procedures involving animals were performed in accordance to guidelines approved by Animal Welfare and Ethical Review Bodies at the University



of Liverpool and University of Glasgow and were carried out in accordance with standard animal housing conditions under local and home office regulations.

**Western blot analysis.** Proteins were extracted from tissue samples as described previously<sup>23</sup>. Briefly, snap frozen tissue samples were homogenised under liquid nitrogen using pestle and mortar. The homogenised tissue was resuspended in buffer containing 20 mM HEPES, 25% glycerol, 0.42 M NaCl, 1.5 mM MgCl<sub>2</sub>, 0.2 mM EDTA, 1 mM DTT, 1 mM PMSF and the following protease inhibitors: aprotinin (2 µg/ml), leupeptin (0.5 µg/ml), pepstatin A (1 µg/ml) and soybean trypsin inhibitor (100 µg/ml), subjected to 3 freeze/thaw cycles and then, following centrifugation, the supernatant was collected and protein concentration determined using a modified Bradford (BioRad, Hemel Hempstead UK). Equal amounts of protein were separated by SDS-PAGE, transferred on to Immobilon™ membranes (Millipore, Fisher Scientific UK Ltd, Loughborough, UK), and Ponceau-S staining was used to verify equivalent protein loading. The membranes were probed with the following antibodies according to established protocol<sup>11</sup>: PKCβII (C-18, Santa Cruz, Insight Biotechnology Ltd, Wembley UK) or HA [clone C29F4, (Cell Signaling Technologies, Hitchin, UK) or clone 16B12 (Covance, Cambridge Bioscience, Cambridge UK)] at a dilution of 1:1,000. Following incubation with secondary HRP-conjugated antibodies, protein bands were visualized using enhanced chemiluminescence (ECL) according to manufacturer's protocol (GE Healthcare Life Sciences, Little Chalfont UK).

**Histopathology and immunohistochemistry.** Splenic tissue was fixed in 10% neutral buffered formalin and then embedded in paraffin. To remove paraffin and rehydrate splenic sections a PT Link device (DAKO, Stockport UK) was used according to the manufacturer's instructions. Immunohistochemical staining was performed using a DAKO Auto-stainer automated slide processing system and the EnVision™ FLEX/HRP kit (DAKO, K8012). The primary antibodies used were PKCβII (C-18) and HA (C29F4). Hematoxylin and eosin (H&E) staining of splenic sections was carried out according to standard protocols.

**Cell preparation.** Peritoneal cells were removed by injecting 5–10 ml ice cold modified PBS (1% BSA + 0.1% Sodium Azide, pH 7.2) into the peritoneal cavity followed by withdrawal of the peritoneal exudates. Spleens were removed and mechanically disrupted to prepare single cell suspensions. Erythrocytes in peripheral blood, peritoneal and splenic samples were lysed by treating with 0.165 M ammonium chloride, prior to washing the cell suspensions.

**Flow cytometry.** Flow cytometry was employed to characterize mature B cell subsets in spleen, peritoneum and peripheral blood comparing Eµ-PKCβII tg mice with wt mice, as indicated. Cells (2–5 × 10<sup>6</sup>) were suspended in 200 µl modified PBS, then antibody cocktails were added and the cell suspension was incubated on ice for 30 min in the dark. Following this the cells were washed with 300 µl modified PBS, and then centrifuged at 2,000 rpm at 4 °C for 2 min. The supernatant was decanted and the pellet was re-suspended in 300 µl modified PBS. Labeled cells were acquired using a LSR-Fortessa flow cytometer (BD Biosciences) and analyzed using FACSDIVA™ and FlowJo™ (BD Biosciences, UK) software packages. Fluorescence-conjugated antibodies were purchased from BioLegend (London, UK) unless otherwise stated: Living Colors™ DsRed mCherry (PT3647-2, Clontech), CD45R/B220-PE (RA3-6B2), CD5-PE/Cy5 (53–7.3), IgD-APC (11-26c.2a), CD43-FITC (S11), IgM-APC/Cy7 (RMM-1), CD21/CD35-PE/Cy7 (7E9), CD24-PerCP/Cy5.5 (M1/69), FITC-Rat IgG2bk Isotype Ctrl (RTK4530) and CD45R/B220-Alexa Fluor™ 488 (RA3-6B2). The percentage of B cell subsets, including FO (IgD<sup>+</sup>IgM<sup>dim</sup>), MZ (IgD<sup>dim</sup>IgM<sup>+</sup>CD43<sup>neg</sup>CD21<sup>+</sup>CD24<sup>+</sup>) and B-1 (B220<sup>+</sup>IgD<sup>dim</sup>IgM<sup>+</sup>CD43<sup>+</sup>CD24<sup>+</sup>) B cell populations were largely similar between wt littermate and non-littermate animals (data not shown), therefore non-littermate and littermate wt mice were considered a single group of wt mice.

**Calcium flux.** Calcium flux analysis in isolated cells was carried out as described previously<sup>24</sup>. Briefly, splenic cells from Eµ-PKCβII tg hom/het mice were labelled with 1 µM Fura-2 AM (Invitrogen Ltd.) in buffer (145 mM NaCl, 5 mM KCl, 1 mM MgSO<sub>4</sub>, 1 mM CaCl<sub>2</sub>, 10 mM HEPES, 0.18% glucose and 0.2% BSA, adjusted to pH 7.4) at 37 °C for 30 min in the dark. Cells were washed, incubated with 10 µg/ml biotinylated anti-IgM for a further 30 min at 4 °C, washed and re-suspended at 1 × 10<sup>6</sup>/ml in buffer. Cells (1.5 × 10<sup>6</sup>) transferred to the fluorimeter cuvette were allowed to warm to 37 °C for 3 min prior to data acquisition. After recording basal fluorescence, 50 µl avidin was added to crosslink the BCR (final concentration 8.3 µg/ml) and recording continued for a further 3 min. Fluorescence was measured at 340 and 380 nm using a Hitachi F-7000 Fluorescence Spectrophotometer (Hitachi High Technologies America, Inc., Schaumburg, IL, USA).

**Ig concentration analysis.** Blood was extracted from mice and serum was prepared by pelleting the RBCs at 12,000g for 10 min. The serum was aliquoted and stored at – 20 °C until needed. Assays of IgM concentration in serum were performed using the LEGENDplex™ kit (BioLegend, UK) following the manufacturers' instructions. IgM concentrations were calculated using the LEGENDplex™ data analysis software dongle.

**Statistical analysis.** All statistical analyses in this study were performed using GraphPad Prism® 8 software.

## Results

**Characterization of Eµ-PKCβII transgenic mice.** Based on the Southern blotting analysis, the number of pEµ-PKCβIIHA-IRES-mCherry transgene copies integrated in the single site of the founder mouse genome was estimated to be greater than one, but less than 10 copies (Fig. 1C). PKCβIIHA expression was then ana-

	Wild type	Std	E $\mu$ -PKC $\beta$ IItg	Std	P value
Spleen weight (mg)	129.4 n = 7	9.02	120.4 n = 9	5.9	0.63
WBC count ( $\times 10^6$ per ml)	3.02 n = 7	0.78	3.74 n = 11	0.62	0.41
<b>B cell/B + T cells</b>					
Spleen	0.60 n = 10	0.046	0.73 n = 13	0.064	0.024
Peritoneum	0.85 n = 6	0.014	0.87 n = 10	0.024	0.25
Peripheral blood	0.71 n = 4	0.063	0.65 n = 10	0.052	0.44

**Table 1.** Comparison of spleen weight, WBC count and B/B + T lymphocyte ratio in E $\mu$ -PKC $\beta$ IItg and wt control mice. B/B + T lymphocyte ratio in spleen, peritoneum and peripheral blood were determined using a FACS-based protocol identifying B cells (B220<sup>+</sup>CD5<sup>-</sup> live lymphocytes) and T cells (B220<sup>-</sup>CD5<sup>+</sup> live lymphocytes). Statistical analysis was performed using a Mann–Whitney U-test.

lysed by Western blot analysis and detected in spleen but not in liver of 6 month-old mice homozygous for the PKC $\beta$ IIHA transgene (hereafter E $\mu$ -PKC $\beta$ IItg mice) (Fig. 1D), suggesting that transgene expression is tissue specific. A comparison of total PKC $\beta$ II expression in protein extracts derived from the splenic tissue showed that PKC $\beta$ II was expressed at significantly higher levels in E $\mu$ -PKC $\beta$ IItg mice compared with wt counterparts (Fig. 1E). In addition, analysis of HA expression within the spleen revealed that expression was concentrated within the follicle area of the peri-arteriolar lymphoid sheaths (PALS) and MZ, both of which are B cell rich areas (Fig. 1F). Although total PKC $\beta$ II expression in the spleen of transgenic and wt mice showed a similar staining pattern, the intensity of staining was always greater in the tissue from transgenic mice where it correlated with that of HA. We were not able to detect the expression of mCherry in E $\mu$ -PKC $\beta$ IItg mice (data not shown). This may be because expression of a secondary gene from an IRES sequence can be variable and not always efficient in transgenic mice and therefore might have been below detection level<sup>25</sup>.

E $\mu$ -PKC $\beta$ IItg mice aged normally and did not show any signs of illness when aged up to 14 months. The WBC count of E $\mu$ -PKC $\beta$ IItg mice was in a normal range and did not differ from that in wt mice (Table 1). In addition, the spleen weight did not change significantly between E $\mu$ -PKC $\beta$ IItg mice and wt mice, and although there appeared a small but significant increased ratio of B cells to combined T/B lymphocytes in the spleen of E $\mu$ -PKC $\beta$ IItg compared to wt mice, this ratio remained similar in the peripheral blood and peritoneum between these animals.

### Splenic tissue from E $\mu$ -PKC $\beta$ IItg mice display an expansion of the MZ B cell population and a concomitant reduction of the FO B cell population.

Although total B cell counts were similar between E $\mu$ -PKC $\beta$ IItg and wt mice, differences were observed between discrete populations. We applied the gating strategy shown in Supplementary Figure 2 for the analysis of B cells within splenic tissue from wt and E $\mu$ -PKC $\beta$ IItg mice. Thus, B220<sup>+</sup> cells were first analysed for surface IgD and IgM expression. E $\mu$ -PKC $\beta$ IItg mice exhibited an increased percentage of IgD<sup>+</sup> IgM<sup>+</sup> B cells and decreased percentage of IgD<sup>+</sup> IgM<sup>dim</sup> B cells compared to wt control mice (Fig. 2A,B). Analysis of the IgD<sup>+</sup> IgM<sup>dim</sup> B cells identified them as mainly FO B cells because of their expression of CD21 and CD24, the phenotype of these cells seemed consistent between wt and E $\mu$ -PKC $\beta$ IItg mice (Supplementary Figure 2), despite lower numbers of these cells in the latter. The IgD<sup>+</sup> IgM<sup>+</sup> B cells were further gated for CD43 expression, and cells negative for this antigen were further analyzed for CD21 and CD24 expression. The major population identified, IgD<sup>+</sup> IgM<sup>+</sup> CD43<sup>neg</sup> CD21<sup>+</sup> CD24<sup>+</sup>, are “MZ-like” in phenotype and resemble a described precursor MZ cell population known as marginal zone precursor B cells<sup>26,27</sup>. This population of “MZ-like” B cells showed significantly greater representation in splenic tissue from E $\mu$ -PKC $\beta$ IItg compared to wt mice, suggesting a strong bias towards this phenotype in the former (Fig. 2C). The bias towards this MZ-like phenotype was further corroborated by H&E stains showing an extended MZ in E $\mu$ -PKC $\beta$ IItg compared with wt mice (Fig. 2D, upper panels), identified by anti-IgM staining (Fig. 2D, lower panels). Interestingly, this is the same area that seemed to stain strongly for PKC $\beta$ II and HA in splenic tissue of transgenic mice (Fig. 1F). Of note, IgD<sup>+</sup> IgM<sup>+</sup> CD24<sup>+</sup> CD43<sup>neg</sup> cells negative for CD21 were present in splenic tissue from E $\mu$ -PKC $\beta$ IItg, but not from wt mice. This population may represent immature B cells but was not further analysed in this study. Functional analysis of splenic B cells from transgenic animals showed that BCR-induced Ca<sup>2+</sup> flux was significantly suppressed in cells isolated from E $\mu$ -PKC $\beta$ IItg mice (Fig. 2E), an observation that is in line with the role of PKC $\beta$  in regulating the function of Btk and PLC $\gamma$ 2-induced calcium release<sup>5</sup>. Thus, these data suggest that B cell-targeted over-expression of PKC $\beta$ II functionally restricts antigen receptor signaling resulting in an expansion of splenic MZ B cells in E $\mu$ -PKC $\beta$ IItg mice.

### The peritoneum of E $\mu$ -PKC $\beta$ II transgenic mice contains an elevated B-1 cell population.

Peritoneal B220<sup>+</sup> B cells exhibited a significant decrease in the percentage of IgD<sup>+</sup> IgM<sup>dim</sup> cells, coupled with significant increase in the percentage of IgD<sup>+</sup> IgM<sup>dim</sup> IgM<sup>+</sup> cells in E $\mu$ -PKC $\beta$ IItg mice when compared to wt mice (Fig. 3A,B, Supplementary Figure 3). Further analyses revealed that the populations of IgD<sup>+</sup> IgM<sup>dim</sup> cells defined by CD24 and CD43 expression were largely similar between wt and E $\mu$ -PKC $\beta$ IItg mice (Supplementary Figure 3). How-

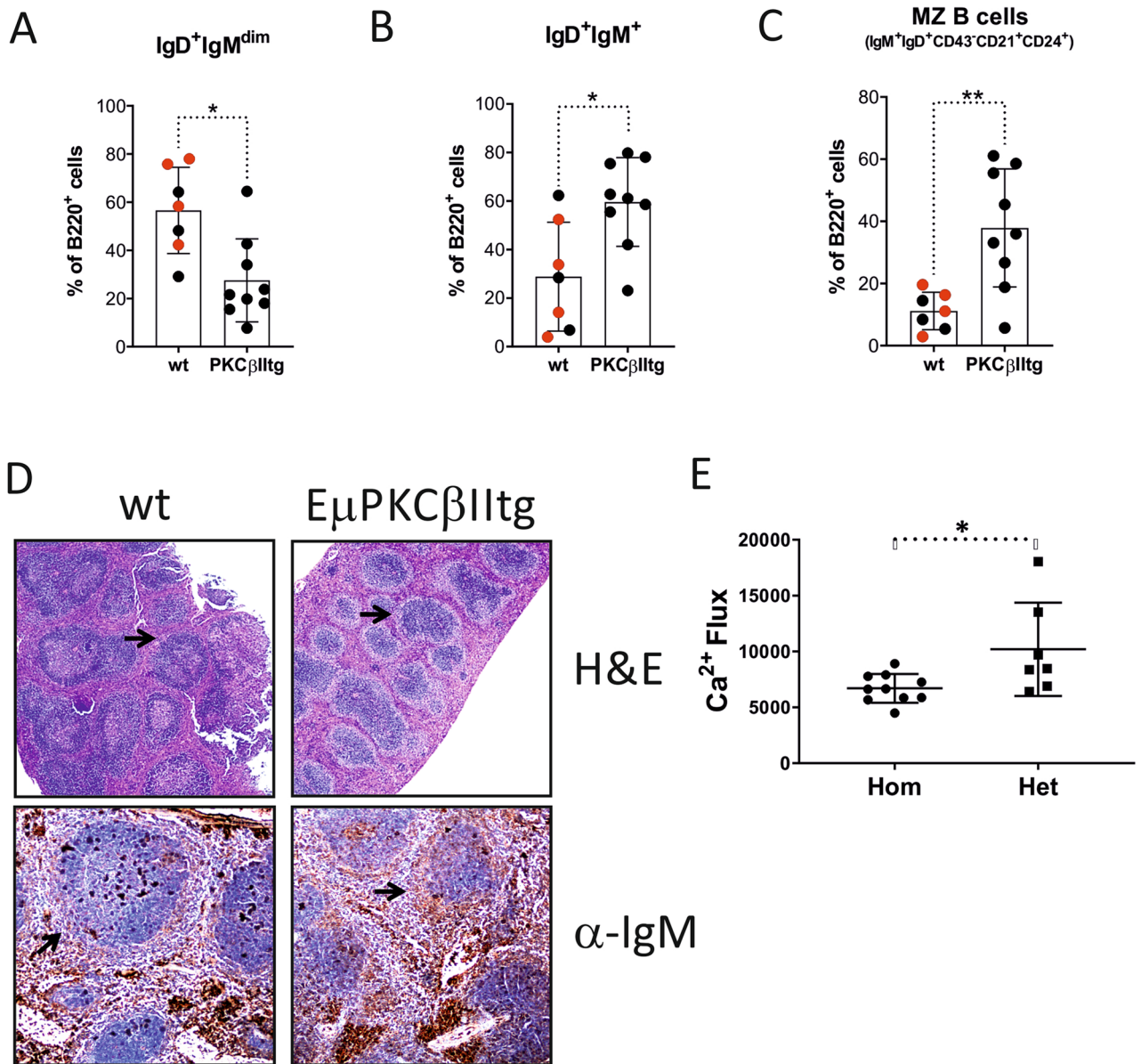


**Figure 2.** Effect of B cell-targeted expression of PKC $\beta$ II on B cell populations in splenic tissue from  $E\mu$ -PKC $\beta$ IItg and wt mice. Single cell suspensions prepared from spleens isolated from  $E\mu$ -PKC $\beta$ IItg and wt mice were stained with a cocktail of antibodies containing B220, IgM, IgD, CD43, CD21 and CD24 markers, and then analysed by flow cytometry. Quantitative comparisons were then made of the percentage B220 $^+$  cells within the following gates (A)  $IgD^+ IgM^{dim}$ , (B)  $IgD^+ IgM^+$ , and (C)  $IgD^+ IgM^+ CD43^- CD21^+ CD24^+$  (MZ-like B cell) for wt and  $E\mu$ -PKC $\beta$ IItg mice as defined by the strategy illustrated in Supplementary Figure 2. Black dots in these graphs refer to wt and homozygous  $E\mu$ -PKC $\beta$ IItg progeny derived from mating heterozygous  $E\mu$ -PKC $\beta$ IItg mice. Red dots refer to wt mice with similar genetic backgrounds (C57BL/6) that are alike in terms of age to the transgenic mice. (D) *upper panels* H&E staining of splenic tissue from wt and  $E\mu$ -PKC $\beta$ IItg mice. *Lower panels* anti-IgM staining of spleen sections from wt and  $E\mu$ -PKC $\beta$ IItg mice. These images are representative of  $n=2$  experiments using splenic tissue from different mice that had been aged in excess of 12 months. Inset arrows indicate MZ. These histogram images have been published in the PhD thesis of AAA<sup>43</sup>. (E) BCR-induced  $Ca^{2+}$  flux in isolated splenic B cells from heterozygous and homozygous  $E\mu$ -PKC $\beta$ IItg mice. Total flux was calculated as area under the curve is reported in arbitrary units. Statistical analysis for parts (A) (\* $P=0.012$ ), (B) (\* $P=0.016$ ), (C) (\*\* $P=0.0052$ ) and (E) (\* $P=0.024$ ) was performed using a Mann–Whitney U test.

ever, similar analysis of  $IgD^{dim} IgM^+$  cells showed that the proportion of  $CD24^+ CD43^+$  cells in  $E\mu$ -PKC $\beta$ IItg mice was significantly increased compared to wt mice (Fig. 3C). These cells carry a B-1 B cell phenotype ( $B220^+ IgM^+ IgD^{dim/-} CD43^+ CD24^{hi}$ ) and are likely to be B-1a cells because the majority of them are also positive for CD5

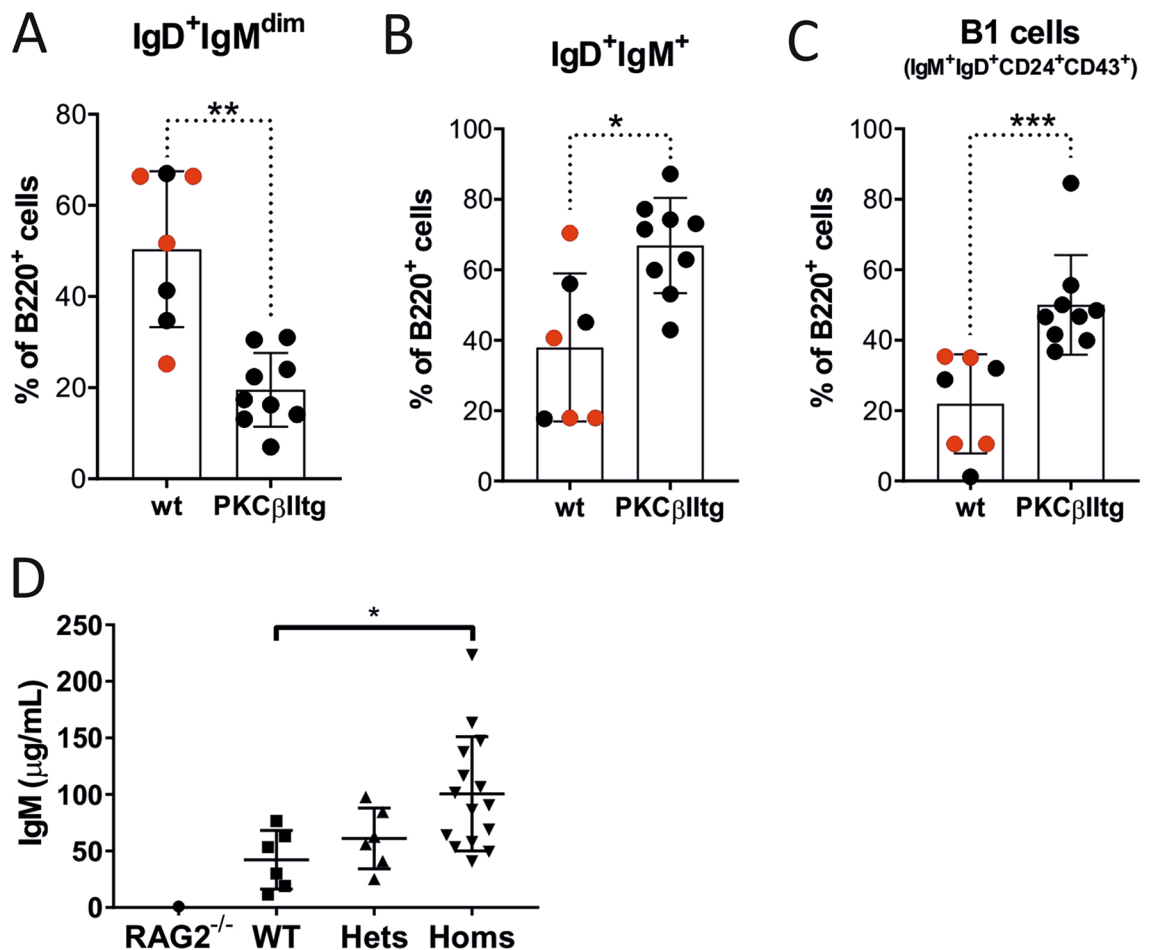


**Figure 3.** Effect of B cell-targeted expression of PKCβII on B cell populations in the peritoneum of Eμ-PKCβIItg and wt mice. Single cell suspensions prepared from peritoneal wash of Eμ-PKCβIItg and wt mice were stained with antibodies to B220, IgM, IgD, CD43, CD24, and CD5 and analyzed by flow cytometry. Quantitative comparisons were then made of the percentage B220<sup>+</sup> cells within the following gates (A) IgD<sup>+</sup>IgM<sup>dim</sup>, (B) IgD<sup>+</sup>IgM<sup>+</sup>, and (C) IgD<sup>dim</sup>IgM<sup>+</sup> CD43<sup>+</sup> CD24<sup>+</sup> (B-1 cells) for wt and Eμ-PKCβIItg mice as defined by the strategy illustrated in Supplementary Figure 3. Black dots in these graphs refer to wt and homozygous Eμ-PKCβIItg progeny derived from mating heterozygous Eμ-PKCβIItg mice. Red dots refer to wt mice with similar genetic backgrounds (C57BL/6) that are alike in terms of age to the transgenic mice. (D) Comparison of IgM levels in serum derived from Rag2 deficient, wt, and heterozygous and homozygous Eμ-PKCβIItg mice. Statistical analysis for parts (A) (\*\*P = 0.0040), (B) (\*P = 0.042), and (C) (\*\*P = 0.0010) was performed using a Mann–Whitney U test, for part (D) analysis was done using a one-way ANOVA and Tukey’s multiple comparisons test (P = 0.040).

(Supplementary Figure 3). Taken together, these results suggest that B cell-targeted over expression of PKCβII results in accumulation of B-1a B cells in the peritoneum of Eμ-PKCβIItg mice.

**Serum IgM levels are increased in Eμ-PKCβIItg mice.** Consistent with the increased proportion of MZ and B-1a cells observed in spleen and peritoneum, Eμ-PKCβIItg mice also exhibited elevated levels of serum IgM compared to wt animals (Fig. 3D). As a negative control we analysed serum derived from a single Rag1<sup>-/-</sup> mouse to show the background of detection for the assay used.

**Peripheral blood from Eμ-PKCβIItg mice contains an expanded population of immature B cells.** When B220<sup>+</sup> B cells derived from peripheral blood were analysed for IgD and IgM expression (Supplementary Figure 4), an expansion of IgD<sup>dim</sup>IgM<sup>+/−</sup> B cells was evident in Eμ-PKCβIItg mice compared to wt mice as was a reduction of IgD<sup>+</sup>IgM<sup>+/−</sup> B cells (Fig. 4). Analysis of CD21 expression on IgD<sup>dim</sup>IgM<sup>+/−</sup> B cells and IgD<sup>+</sup>IgM<sup>+/−</sup> B cells from Eμ-PKCβIItg and wt mice showed that the former were CD21<sup>neg</sup> while the latter were CD21<sup>+</sup> (Supplementary Figure 4). As CD21 is a marker of B cell maturity<sup>28</sup>, the lack of CD21 expression on IgD<sup>dim</sup>IgM<sup>+/−</sup> B cells from Eμ-PKCβIItg mice suggests that these cells are most likely immature B cells. Considering that the WBC and the B: T ratio in peripheral blood is not significantly different between Eμ-PKCβIItg and wt mice (Table 1), these results suggest that B cell-directed expression of PKCβII results in a shift towards expansion of the immature B cell population in peripheral blood.

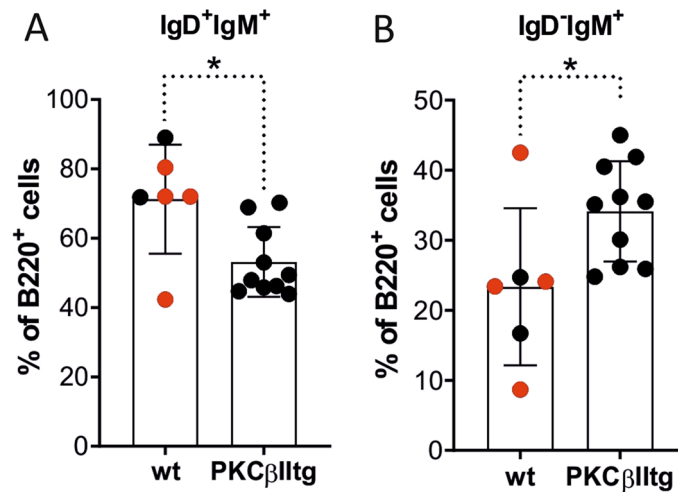


**Figure 4.** Effect of B cell-targeted expression of PKC $\beta$ II on B cell populations in peripheral blood of E $\mu$ -PKC $\beta$ IItg and wt mice. Single cell suspensions prepared from peripheral blood and bone marrow of E $\mu$ -PKC $\beta$ IItg and wild type mice were stained with antibodies to B220, IgM, IgD, and CD21 and analyzed by flow cytometry. Quantitative comparisons were then made of the percentage B220<sup>+</sup> cells within the following gates (A) IgD<sup>+</sup> IgM<sup>+</sup>, and (B) IgD<sup>dim</sup> IgM<sup>+</sup> for wt and E $\mu$ -PKC $\beta$ IItg mice as defined by the strategy illustrated in Supplementary Figure 4. Black dots in these graphs refer to wt and homozygous E $\mu$ -PKC $\beta$ IItg progeny derived from mating heterozygous E $\mu$ -PKC $\beta$ IItg mice. Red dots refer to wt mice with similar genetic backgrounds (C57BL/6) that are alike in terms of age to the transgenic mice. Statistical analysis for parts (A) (\*P = 0.030) and (B) (\*P = 0.023) was performed using a Mann–Whitney U test.

## Discussion

Upregulated expression of PKC $\beta$ II is frequently observed in the malignant cells of B lymphoproliferative diseases<sup>29</sup>, and, in particular, CLL where its overexpression is a phenotypic feature<sup>11</sup>. Because of this, we aimed to analyze the effect of PKC $\beta$ II overexpression on the B cell compartment by generating a transgenic mouse strain where expression of PKC $\beta$ II was driven by the E $\mu$  promoter. Consistent with our initial hypothesis, the consequence of B cell-directed PKC $\beta$ II overexpression is a proportional change in FO, MZ-like, B-1 and immature B cell populations respectively in the spleen, peritoneum and peripheral blood of E $\mu$ -PKC $\beta$ IItg mice. Further examination of the E $\mu$ -PKC $\beta$ IItg mice shows suppression of BCR signaling in splenic B cells, and elevated levels of serum IgM. Although expansion of the B-1 cell compartment is a feature of several mouse models of CLL<sup>15–19</sup>, we did not observe disease in E $\mu$ -PKC $\beta$ IItg mice and the proportion of B cells to combined B/T cells (taken as total lymphocytes) in these animals remained largely similar to that of wt mice despite aging them for 15 months. We conclude that PKC $\beta$ II plays an important role in B cell development, with overexpression resulting in biased MZ-like and B-1 B cell development, but not in the pathogenesis of a CLL-like or other B lymphoproliferative disease in E $\mu$ -PKC $\beta$ IItg mice.

A limitation of this study is that our findings are based on data generated from analysis of animals that were derived from a single founder that was minimally backcrossed into the parental strain. The phenotype we describe could therefore potentially be a result of positional effect or an unidentified factor involved in producing the E $\mu$ -PKC $\beta$ IItg mice. However, comparison of B cell phenotypes within spleen, peritoneum and peripheral blood from the wt mice we analyzed are similar between littermate and non-littermate (i.e. C57BL/6 background) wt animals. These findings indicate that the genetic background of the strains used to generate E $\mu$ -PKC $\beta$ IItg mice had little, if any, effect on our observations. Furthermore, the phenomenon we observe is consistent with a mechanism whereby higher expression of PKC $\beta$ II within B cells of E $\mu$ -PKC $\beta$ IItg mice could limit BCR signaling by suppressing Btk activation. A well-described role of PKC $\beta$  in B cells is the phosphorylation of the S<sup>180</sup> residue in Btk leading to downregulation of its function<sup>4,5,30</sup>. Our own work shows that overexpressed PKC $\beta$ II in primary CLL cells limits BCR signaling in the presence of pS<sup>180</sup><sup>11,31</sup>. The novel mouse model we describe herein recapitulates these findings and we show that BCR signaling in B cells from E $\mu$ -PKC $\beta$ IItg mice is suppressed. In contrast, a study describing the phenotype of PKC $\beta$  knockout mice showed enhanced BCR-mediated signaling in B cells from these animals<sup>4</sup>, a phenomenon similar to that observed in a study of PKC $\beta$  inhibition on BCR signaling<sup>32</sup>. This same study also showed that MZ and B1 B cell populations, as well as serum IgM levels were severely reduced in PKC $\beta$  knockout mice<sup>4</sup>. Together, these observations provide support to our interpretation that suppressed BCR signaling resulting from targeted PKC $\beta$ II overexpression in E $\mu$ -PKC $\beta$ IItg mice leads to expansion of MZ-like and B1 B cells within total B cell populations and increased serum IgM levels. Further complementary support can be found in our observation that splenic B cell populations are slightly increased in E $\mu$ -PKC $\beta$ IItg mice, whilst Leitges et al.<sup>4</sup> observed a slight decrease in these populations in their PKC $\beta$  knockout mice. Taken together, these observations suggest that the phenotype we observe is most likely due to transgenic overexpression of PKC $\beta$ II rather than a confounding factor.



In the current study we have focused on PKC $\beta$ II and have not considered its splice variant PKC $\beta$ I. Since we have not silenced the expression of the gene that codes for PKC $\beta$  in our system, we cannot rule out the contribution of PKC $\beta$ I to the phenotype we have generated. Future studies crossing the E $\mu$ -PKC $\beta$ IItg mouse with a PKC $\beta$  null mouse would enable us to determine the role of PKC $\beta$ II in B cells more precisely.

It is intriguing that despite the noted lineage biases observed in B cell populations in the E $\mu$ -PKC $\beta$ IItg mice, aged animals did not develop a disease endpoint. A possible reason for this could be that overexpression of PKC $\beta$ II alone is not sufficient to drive the pathogenesis in B lymphoid diseases. However, E $\mu$ -PKC $\beta$ IItg mice may be more susceptible to the development of these diseases since it has been demonstrated that, for example, in colon cancer, overexpression of PKC $\beta$ II promotes development of disease by increasing the sensitivity of colonic epithelial cells to carcinogenic stimuli<sup>33,34</sup>. Indeed, this may be particularly relevant for CLL because this disease appears to develop from a lymphocytosis of B-1 cells in both mice and humans<sup>14–17</sup>. If this hypothesis is correct, E $\mu$ -PKC $\beta$ IItg mice crossed with another mouse model of CLL, such as the Tcl-1 model, would exhibit accelerated development of disease because of the expanded population of B-1 cells. An alternative reason for the lack of disease development may be that the expression levels of PKC $\beta$ II achieved in our mouse model are not high enough to facilitate neoplastic transformation. Our previous work in CLL showed that the malignant cells in this disease express up to sevenfold greater amounts of this PKC isozyme than do normal B cells<sup>17</sup>. In the current study we were only able to achieve an approximate twofold increase of PKC $\beta$ II in E $\mu$ -PKC $\beta$ IItg compared to wt mice.

We propose that the modest increase in protein levels of PKC $\beta$ II observed in E $\mu$ -PKC $\beta$ IItg mice alters BCR signaling resulting in skewed representation of B cell population subsets in the periphery with expansion of MZ-like cells, B-1 B cells and immature B cells as we describe in this study. PKC $\beta$ II in B cells has two key targets; CARMA1 (CARD11) which, when phosphorylated, combines with MAL1 and Bcl10 to form a complex that recruits TAK1 to stimulate activation of the NF $\kappa$ B and JNK signaling pathways and promote cell survival<sup>35–37</sup>, and Btk where S<sup>180</sup> phosphorylation downregulates its function as discussed above<sup>5</sup>. Hence, overexpression of PKC $\beta$ II will preserve survival of B cells while limiting their ability to respond to BCR engagement. Such limitation is likely to affect B cell differentiation and our observations can be explained by the "strength of signal" model suggested by Cariappa et al.<sup>38,39</sup> where transitional B cells in the periphery respond to strong or "triggered" signals delivered via the BCR with commitment to FO B cell differentiation, while weaker or "tickled" BCR signals lead to differentiation towards MZ and B-1 B cells. The absence of BCR signals results in cell death due to neglect. This is likely the explanation for the phenotype of the MZ-like B cells we identify. These cells possess similarity to MZ precursor B cells<sup>26</sup>, the presence of which are directly related to BCR signaling strength as is demonstrated in Aiolos- and CD22-deficient mice<sup>27,38,40</sup>. Weakening of BCR signaling by overexpression of PKC $\beta$ II is also likely to be responsible for the increased number of immature B cells in peripheral blood we observe in E $\mu$ -PKC $\beta$ IItg mice. Elimination of self-reactive B cell clones occurs at the pre-B cell stage within bone marrow, and is achieved either by receptor editing whereby B cell development is arrested while further gene rearrangements occur in order to mitigate self-reactivity<sup>41</sup>, or by the induction of apoptosis by strong BCR signals<sup>42</sup>. Since both of these processes are driven by Btk<sup>8</sup>, overexpression of PKC $\beta$ II within pre-B cells of E $\mu$ -PKC $\beta$ IItg mice could limit strong self-antigen-driven BCR signaling by suppressing Btk activation thus generating the increased numbers of immature B cells seen here. We propose that the modestly increased levels of PKC $\beta$ II in E $\mu$ -PKC $\beta$ IItg mice alters BCR signaling such that B cell subsets become skewed in the periphery as demonstrated; populations of MZ-like cells, B-1 B cells and immature B cells all expand<sup>5,8,26,27,35–42</sup>.

In conclusion, we have generated a transgenic mouse strain with targeted overexpression of PKC $\beta$ II within B lineage cells; E $\mu$ -PKC $\beta$ IItg. We show that the phenotype associated with E $\mu$ -PKC $\beta$ IItg mice skews development of MZ-like and immature B cells over FO B cells in the spleen and peripheral blood, and of B-1 B cells in the peritoneum, thereby providing *in vivo* data that support our hypothesis that overexpression of PKC $\beta$ II might result in an expansion of B1 and MZ B cell populations. Considering the phenotype of the PKC $\beta$  knockout mouse<sup>3</sup>, we have speculated that the increased populations of MZ-like and B-1a cells within the E $\mu$ -PKC $\beta$ IItg mouse would generate a phenotype where IgM antibodies would be prevalent and this was indeed the case. Thus, we have demonstrated that PKC $\beta$ II specifically plays an important role in B cell development in mice. This novel mouse strain may be useful in studies of diseases involving BCR signaling, and, in particular, CLL.

Received: 19 June 2019; Accepted: 21 July 2020

Published online: 04 August 2020

## References

1. Burger, J. A. & Wiestner, A. Targeting B cell receptor signalling in cancer: Preclinical and clinical advances. *Nat. Rev. Cancer* **18**, 148–167 (2018).
2. Yam-Puc, J., Zhang, L., Zhang, Y. & Toellner, K. Role of B-cell receptors for B-cell development and antigen-induced differentiation. *F1000Research* **7**, (2018).
3. Spitaler, M. & Cantrell, D. A. Protein kinase C and beyond. *Nat. Immunol.* **5**, 785–790 (2004).
4. Leitges, M. *et al.* Immunodeficiency in protein kinase c $\beta$ -deficient mice. *Science* **273**, 788–791 (1996).
5. Kang, S. W. *et al.* PKC $\beta$  modulates antigen receptor signaling via regulation of Btk membrane localization. *EMBO J.* **20**, 5692–5702 (2001).
6. Kerner, J. D. *et al.* Impaired expansion of mouse B cell progenitors lacking Btk. *Immunity* **3**, 301–312 (1995).
7. Khan, W. N. *et al.* Defective B-cell development and function in Btk-deficient mice. *Immunity* **3**, 283–299 (1995).
8. Maas, A. & Hendriks, R. W. Role of Bruton's tyrosine kinase in B cell development. *Dev. Immunol.* **8**, 171–181 (2001).
9. Coussens, L., Rhee, L., Parker, P. J. & Ullrich, A. Alternative splicing increases the diversity of the human protein kinase C family. *DNA* **6**, 389–394 (1987).

10. Kubo, K., Ohno, S. & Suzuki, K. Primary structures of human protein kinase C beta I and beta II differ only in their C-terminal sequences. *FEBS Lett.* **223**, 138–142 (1987).
11. Abrams, S. T. *et al.* B-cell receptor signaling in chronic lymphocytic leukemia cells is regulated by overexpressed active protein kinase C $\beta$ II. *Blood* **109**, 1193–1201 (2007).
12. Holler, C. *et al.* PKC $\beta$  is essential for the development of CLL in the TCL1 transgenic mouse model: Validation of PKC $\beta$  as a therapeutic target in CLL. *Blood* **113**, 2791–2794 (2009).
13. Chiorazzi, N. & Ferrarini, M. Cellular origin(s) of chronic lymphocytic leukemia: Cautionary notes and additional considerations and possibilities. *Blood* **117**, 1781–1791 (2011).
14. Seifert, M. *et al.* Cellular origin and pathophysiology of chronic lymphocytic leukemia. *J. Exp. Med.* **209**, 2183–2198 (2012).
15. Bichi, R. *et al.* Human chronic lymphocytic leukemia modeled in mouse by targeted TCL1 expression. *Proc. Natl. Acad. Sci. USA* **99**, 6955–6960 (2002).
16. Klein, U. *et al.* The DLEU2/miR-15a/16-1 cluster controls B cell proliferation and its deletion leads to chronic lymphocytic leukemia. *Cancer Cell* **17**, 28–40 (2010).
17. Planelles, L. *et al.* APRIL promotes B-1 cell-associated neoplasm. *Cancer Cell* **6**, 399–408 (2004).
18. Santanam, U. *et al.* Chronic lymphocytic leukemia modeled in mouse by targeted miR-29 expression. *Proc. Natl. Acad. Sci. USA* **107**, 12210–12215 (2010).
19. Michie, A. M., Nakagawa, R. & McCaig, A. M. Murine models for chronic lymphocytic leukaemia. *Biochem. Soc. Trans.* **035**, 1009–1012 (2007).
20. Shanafelt, T. D., Ghia, P., Lanasa, M. C., Landgren, O. & Rawstron, A. C. Monoclonal B-cell lymphocytosis (MBL): Biology, natural history and clinical management. *Leukemia* **24**, 512–520 (2010).
21. Shaw, A. C., Swat, W., Ferrini, R., Davidson, L. & Alt, F. W. Activated Ras signals developmental progression of recombina-activating gene (RAG)-deficient pro-B lymphocytes. *J. Exp. Med.* **189**, 123–129 (1999).
22. Kim, K. J., Kanellopoulos-Langevin, C., Merwin, R. M., Sachs, D. H. & Asofsky, R. Establishment and characterization of BALB/c lymphoma lines with B cell properties. *J. Immunol.* **122**, 549–554 (1979).
23. Athwal, T. *et al.* Expression of human cationic trypsinogen (PRSS1) in murine acinar cells promotes pancreatitis and apoptotic cell death. *Cell Death Dis.* **5**, e1165 (2014).
24. McCaig, A. M., Cosimo, E., Leach, M. T. & Michie, A. M. Dasatinib inhibits B cell receptor signalling in chronic lymphocytic leukaemia but novel combination approaches are required to overcome additional pro-survival microenvironmental signals. *Br. J. Haematol.* **153**, 199–211 (2011).
25. Kozak, M. A second look at cellular mRNA sequences said to function as internal ribosome entry sites. *Nucleic Acids Res.* **33**, 6593–6602 (2005).
26. Srivastava, B., Quinn, W. J. III., Hazard, K., Erikson, J. & Allman, D. Characterization of marginal zone B cell precursors. *J. Exp. Med.* **202**, 1225–1234 (2005).
27. Pillai, S. & Cariappa, A. The follicular versus marginal zone B lymphocyte cell fate decision. *Nat. Rev. Immunol.* **9**, 767–777 (2009).
28. Allman, D. & Pillai, S. Peripheral B cell subsets. *Curr. Opin. Immunol.* **20**, 149–157 (2008).
29. Decouvelaere, A. V., Morschhauser, F., Buob, D., Copin, M. C. & Dumontet, C. Heterogeneity of protein kinase C  $\beta$ 2 expression in lymphoid malignancies. *Histopathology* **50**, 561–566 (2007).
30. Liu, C. *et al.* A negative-feedback function of PKC $\beta$  in the formation and accumulation of signaling-active B cell receptor micro-clusters within B cell immunological synapse. *J. Leuk. Biol.* **97**, 887–900 (2015).
31. Abrams, S. T., Brown, B. R. B., Zuzel, M. & Slupsky, J. R. Vascular endothelial growth factor stimulates protein kinase C $\beta$ II expression in chronic lymphocytic leukaemia cells. *Blood* **115**, 4447–4454 (2010).
32. Venkataraman, C. *et al.* Selective role of PKC $\beta$  enzymatic function in regulating cell survival mediated by B cell antigen receptor cross-linking. *Immunol. Lett.* **105**, 83–89 (2006).
33. Gökmen-Polar, Y., Murray, N. R., Velasco, M. A., Gatalica, Z. & Fields, A. P. Elevated protein kinase C $\beta$ II is an early promotive event in colon carcinogenesis. *Cancer Res.* **61**, 1375–1381 (2001).
34. Murray, N. R. *et al.* Overexpression of protein kinase C $\beta$ II induces colonic hyperproliferation and increased sensitivity to colon carcinogenesis. *J. Cell Biol.* **145**, 699–711 (1999).
35. Shinohara, H., Maeda, S., Watarai, H. & Kurosaki, T. I $\kappa$ B kinase beta-induced phosphorylation of CARMA1 contributes to CARMA1 Bcl10 MALT1 complex formation in B cells. *J. Exp. Med.* **204**, 3285–3293 (2007).
36. Shinohara, H. *et al.* PKC beta regulates BCR-mediated IKK activation by facilitating the interaction between TAK1 and CARMA1. *J. Exp. Med.* **202**, 1423–1431 (2005).
37. Su, T. T. *et al.* PKC- $\beta$  controls I $\kappa$ B kinase lipid raft recruitment and activation in response to BCR signaling. *Nat. Immunol.* **3**, 780–786 (2002).
38. Cariappa, A. *et al.* The Follicular versus marginal zone B lymphocyte cell fate decision is regulated by Aiolos, Btk, and CD21. *Immunity* **14**, 603–615 (2001).
39. Bowers, E. M. *et al.* Virtual ligand screening of the p300/CBP histone acetyltransferase: Identification of a selective small molecule inhibitor. *Chem. Biol.* **17**, 471–482 (2010).
40. Samardzic, T. *et al.* Reduction of marginal zone B cells in CD22-deficient mice. *Eur. J. Immunol.* **32**, 561–567 (2002).
41. Gay, D., Saunders, T., Camper, S. & Weigert, M. Receptor editing: An approach by autoreactive B cells to escape tolerance. *J. Exp. Med.* **177**, 999–1008 (1993).
42. Nemazee, D. A. & Burki, K. Clonal deletion of B lymphocytes in a transgenic mouse bearing anti-MHC class I antibody genes. *Nature* **337**, 562–566 (1989).
43. Azar, A. A. *Generation of PKC $\beta$ II transgenic mice for the study of chronic lymphocytic leukaemia* Ph.D. thesis, University of Liverpool (2013).

## Acknowledgements

The authors would like to acknowledge the assistance provided by the Flow Cytometry and Cell Sorting Facility and Biological Services Units of the University of Liverpool and the University of Glasgow. JRS was in receipt of LLR funding (Ref 13013). AMM was in receipt of LLR funding (Ref. 13012). The experiments reported here also feature in the doctoral thesis of AAA<sup>43</sup>. This paper is dedicated to Dr Ferahim A. Azar.

## Author contributions

A.A.A. designed the study, performed experiments, analyzed data and wrote the paper. A.M.M., A.T., N.M., G.K.M. and K.J.T. performed experiments and analyzed data. J.R.S. and N.V. designed the study, performed experiments, analyzed data and wrote the paper.

### Competing interests

JRS has received funding from Verastem Inc., and has a collaborative relationship with the Netherlands Translational Research Center B.V. The other authors of this manuscript have no potential competing interests.

### Additional information

**Supplementary information** is available for this paper at <https://doi.org/10.1038/s41598-020-70191-y>.

**Correspondence** and requests for materials should be addressed to N.V. or J.R.S.

**Reprints and permissions information** is available at [www.nature.com/reprints](http://www.nature.com/reprints).

**Publisher's note** Springer Nature remains neutral with regard to jurisdictional claims in published maps and institutional affiliations.



**Open Access** This article is licensed under a Creative Commons Attribution 4.0 International License, which permits use, sharing, adaptation, distribution and reproduction in any medium or format, as long as you give appropriate credit to the original author(s) and the source, provide a link to the Creative Commons license, and indicate if changes were made. The images or other third party material in this article are included in the article's Creative Commons license, unless indicated otherwise in a credit line to the material. If material is not included in the article's Creative Commons license and your intended use is not permitted by statutory regulation or exceeds the permitted use, you will need to obtain permission directly from the copyright holder. To view a copy of this license, visit <http://creativecommons.org/licenses/by/4.0/>.

© The Author(s) 2020